Inversin relays Frizzled-8 signals to promote proximal pronephros development

Soeren Lienkamp[a], Athina Ganner[a], Christopher Boehlke[a], Thorsten Schmidt[b], Sebastian J. Arnold[a], Tobias Schäfer[a], Daniel Romaker[a], Julia Schuler[a], Sylvia Hoff[a,c], Christian Powelske[a], Annekathrin Eifler[a], Corinna Krönig[a], Axel Bullerkotte[a], Roland Nitschke[d,e], E. Wolfgang Kuehn[a], Emily Kim[a], Hans Burkhardt[b,e], Thomas Brox[e,f], Olaf Ronneberger[b,e], Joachim Gloy[a], and Gerd Walz[a,e,1]

[a]Renal Division, Department of Medicine, University Hospital Freiburg, 79106 Freiburg, Germany; [b]Chair of Pattern Recognition and Image Processing, Institute for Computer Science, University of Freiburg, 79104 Freiburg, Germany; [c]Faculty of Biology, University of Freiburg, 79104 Freiburg, Germany; [d]Center for Biological Systems Analysis, Life Imaging Center, 79104 Freiburg, Germany; [e]Center for Biological Signaling Studies (BIOSS), 79104 Freiburg, Germany; and [f]Department of Electrical Engineering and Computer Sciences, University of California, Berkeley, CA 94720-1758

Mutations of *inversin* cause type II nephronophthisis, an infantile autosomal recessive disease characterized by cystic kidney disease and developmental defects. Inversin regulates Wnt signaling and is required for convergent extension movements during early embryogenesis. We now show that Inversin is essential for *Xenopus* pronephros formation, involving two distinct and opposing forms of cell movements. Knockdown of Inversin abrogated both proximal pronephros extension and distal tubule differentiation, phenotypes similar to that of *Xenopus* deficient in Frizzled-8. Exogenous Inversin rescued the pronephric defects caused by lack of Frizzled-8, indicating that Inversin acts downstream of Frizzled-8 in pronephros morphogenesis. Depletion of Inversin prevents the recruitment of Dishevelled in response to Frizzled-8 and impeded the accumulation of Dishevelled at the apical membrane of tubular epithelial cells in vivo. Thus, defective tubule morphogenesis seems to contribute to the renal pathology observed in patients with nephronophthisis type II.

renal development | Wnt/PCP signaling

Inversin (Invs, NPHP2) acts as a molecular switch between canonical and noncanonical Wnt signaling (1, 2). Inversin inhibits the canonical Wnt pathway by targeting cytoplasmic Dishevelled for degradation. Inversin is also involved in noncanonical Wnt signaling. Inversin contains multiple ankyrin repeats and shares the domain architecture with the *Drosophila* protein Diego, a known planar cell polarity (PCP) protein. Both Inversin and Diego interact with Dishevelled (Dvl), Strabismus (Stbm), and Prickle (Pk) (3–5). Recruitment of Dishevelled to the plasma membrane after Frizzled activation is a key event in noncanonical Wnt signaling (6, 7). Inversin colocalizes with Dishevelled at the membrane of polarized renal epithelial cells (5), suggesting that Inversin plays a role in noncanonical Wnt signaling in the kidney.

Nephronophthisis (NPH) is the most frequent genetic cause of renal failure in children and young adults. The youngest group consists of children with *Inversin* mutations, whose renal failure occurs between birth and 3 y of age (infantile form, NPH type II). Renal abnormalities in NPH include tubular basement membrane disruption, tubular atrophy, and formation of cysts that are typically aligned along the cortico-medullary border (8). The inversion of embryo-turning (*inv*) mouse, lacking exons 4–11 of *inversin*, dies from renal and/or hepatic failure shortly after birth. The kidneys display an unusual persistence of tubular narrowing and dilatation (5, 9, 10). However, the precise role of Inversin in early renal development is still elusive.

To overcome the limitations of studying mammalian organogenesis (11), we analyzed *Xenopus laevis* pronephros development by intravital microscopy. In contrast to the rudimentary pronephric structure in mammals, the amphibian pronephros serves as a functional excretory organ during the earliest stages of development. Each of the paired organs is made up of a single nephron, a functional unit consisting of the glomus, where the blood is filtered into the coelomic cavity, and one tubule, through which the primary urine passes to be excreted through the cloaca (12); the simple architecture and morphological and physiological similarities to the more complex meso- and metanephros make it an ideal model to study early renal development (13). The pronephros originates from the intermediate mesoderm and is patterned in a proximal to distal fashion after the nephrogenic mesenchyme condensates into an epithelialized tubule (14–16). Morphogenesis of the early pronephros has been studied in *Xenopus* by vital dye injections or transplantation assays (17). These studies show that the segregation of the pronephric duct from the intermediate mesoderm is followed by cell migration in a caudal direction before the duct fuses with the rectal diverticulum.

The analysis of Wnt9b-deficient mice underlined the importance of the noncanonincal Wnt/PCP signaling pathway for renal development (18). Similarly, Frizzled-8 depletion in the *Xenopus* pronephros disrupts tubule differentiation without affecting early pronephros specification (19).

In this study, we analyzed the role of Inversin during renal development in *X. laevis* using confocal time-lapse imaging of intact embryos. We observed two opposing morphogenetic cell movements that extend the proximal pronephric tubule in a ventral direction. Inversin is essential for the morphogenesis of the proximal and intermediate pronephric system and relays Frizzled-8–dependent signals to recruit Dishevelled to the plasma membrane. Depletion of Inversin leads to impaired ventral extension and elongation of the early pronephros.

Results

Inversin Is Required for Normal Pronephros Development. To investigate the role of Inversin during pronephros development in *X. laevis*, we depleted endogenous Inversin using targeted injections of a translation-blocking morpholino antisense oligonucleotide (Invs-Mo) (Fig. S1 *A–C*). When bilateral injections were targeted to the blastomeres that mainly contribute to the pronephros (V2), embryos developed pronounced edema at stages 43–45 (Fig. 1 *A* and *B*) as a possible consequence of im-
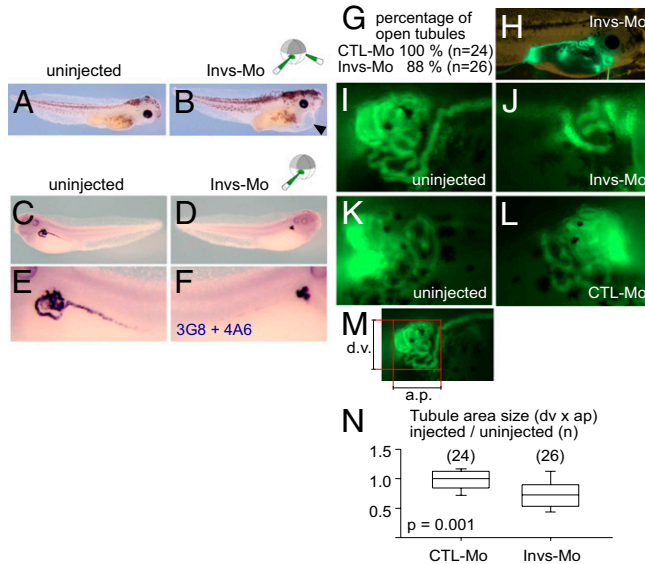
Fig. 1. Inversin is required for pronephric tubule development in *X. laevis*. (*A* and *B*) Bilateral injection of Invs-Mo at the four-cell stage resulted in severe edema. (*C*) The pronephros-specific antibodies 3G8 and 4A6 stain the entire pronephric tubule on the uninjected side. (*D*) On the Invs-Mo–injected side of the same embryo, staining is absent in the distal and intermediate tubule segment but is maintained in the proximal segment. (*E* and *F*) Enlarged view of the pronephros in *C* and *D*, respectively. (*G*) Percentages of embryos with unobstructed tubular excretion on both sides. (*H*) Fluorescent dextran (70 kDa) excretion shows tubule patency in Invs-Mo–injected embryos. (*I–L*) Enlarged views of the pronephros at the phase of maximal dextran excretion. Note the reduction in tubular coiling on the Invs-Mo–injected side (*J*) compared with the uninjected side (*I*). (*K* and *L*) Injection of control-Mo (CTL-Mo) did not interfere with tubule patency or length. (*M*) Tubule-area size was measured as depicted. d.v., dorso-ventral; a.p., anterior-posterior. (*N*) Ratios of injected vs. uninjected tubule areas of the same embryos.

paired pronephric function (20). Whole-mount immunostainings with the tubule-specific antibodies 4A6 and 3G8 (14) outlined the entire pronephric tubule of the uninjected side at stage 40 (Fig. 1*E*) but only the most proximal tubules in unilaterally Invs-Mo–injected embryos (Fig. 1*F*). To determine whether the integrity of the tubule was impaired, we performed a dye excretion assay. Within seconds after injection into the coelomic cavity, fluorescent dextran (70 kDa) was secreted through the pronephros (Fig. 1*H*). At stage 42, the vast majority of Invs-Mo–injected embryos maintained a patent pronephros (88%; *n* = 26) (Fig. 1*G*). Interestingly, the coiled lumen of the proximal tubules marked by fluorescence seemed reduced in total volume on the Invs-Mo–injected side (Fig. 1*J*). We calculated the area occupied by the pronephric tubules by measuring the maximal dorso-ventral and cranio-caudal distance of tubular coiling (Fig. 1*M*). The ratio between injected and uninjected sides confirmed that the pronephric loops occupied a significantly smaller area on the Invs-Mo–injected side (57% of the uninjected side) (Fig. 1*N*). Standard control Mo (CTL-Mo) injections did not affect the tubule area (98% of the uninjected side). Thus, Inversin depletion does not affect the formation of the pronephric lumen or fusion of the pronephric duct with the rectal diverticulum, but it limits the extension of the pronephric tubule, resulting in a shortened and simplified tubular convolute.

Inversin Is Required for Tubule Elongation. The β1 subunit of the Na-K-ATPase (*atp1a1*), specifically expressed in the early pronephros (21), was visualized by in situ hybridization. After condensation of the lateral mesoderm, the primary pronephric loop begins to extend ventrally (Fig. S2*C*) and subsequently, forms the pronephric

tubule (Fig. S2*G*). In Invs-Mo–injected embryos, the extension of the primary loop was reduced at stage 34 (Fig. S2*D*), resulting in a stunted pronephros at stage 40 compared with the uninjected side. Despite the lack of ventral pronephros extension, simplified tubules formed in the absence of Inversin (Fig. S2*J*), suggesting that Inversin plays an important role in ventral extension of the pronephric tubules during early renal morphogenesis. Abnormal tubulogenesis was also observed in E17.5 kidneys of $inv^{(-/-)}$ mice. At this stage, in situ hybridization for ClC-K_a on serial sections produced a strong and reliable signal, which was used to reconstruct the ascending limbs and early distal tubules (Fig. S2 *K–L*). $inv^{(-/-)}$ kidneys tended to have fewer tubules [Inv$^{(-/-)}$ = 132.5 ± 16.8 vs. wild type (WT) = 150 ± 8.9; mean ± SEM; *n* = 4 kidneys)] that were on average shorter than in WT or heterozygote littermates (Fig. S2*M*) (*P* = 0.057).

Several transcription factors mark the pronephros anlagen (22–25). Whole-mount in situ hybridization for LIM homeobox 1 (Lim-1) (*lhx1*), paired box 8 (*pax8*), hepatocyte nuclear factor 1 homeobox B (vHNF1-1) (*hnf1β*), and GATA binding protein 3 (*gata3*) did not uncover any effect of Inversin depletion on renal primordia. Wnt-4 (*wnt4*) expression was not affected as detected by in situ hybridization. (Fig. S3 *A–N* and Table S1). The simplified tubules observed after Inversin knockdown led us to investigate pronephros segmentation at stage 38 (13, 21) (Fig. S4*A*). In situ hybridization against the sodium/glucose cotransporter (xSGLT-1K) (*slc5a1*), the sodium bicarbonate cotransporter 1 (NBC1) (*slc4a4*), the sodium/potassium/chloride transporter (NKCC2) (*slc12a1*), the chloride channel K (ClC-K) (*clcnkb*), and Nephrin (*nphs*) showed that all markers were present in Invs-Mo–injected embryos (Fig. S4 *B–M*), indicating that Inversin does not interfere with glomus maturation or pronephros segmentation. However, the intermediate segment, albeit present, was shortened in Invs-Mo–injected embryos (Fig. S4 *F, G, J, and K*). To quantify these defects, we measured the dorso-ventral extension of the tubule after in situ hybridization for ClC-K and found a reduction in size of 44% compared with the uninjected side (0.202–0.113 mm; *n* = 59) (Fig. S4*N*). Coinjection of a murine *Inversin* mRNA rescued this phenotype and reduced the difference to 11% (0.189–0.168 mm; *n* = 50), confirming the specificity of the Invs-Mo–mediated depletion of Inversin. Defective in situ staining patterns for the distal tubule markers NBC1 (reduced in 56% of injected embryos) and the thiazide-sensitive NaCl cotransporter (NCC2) (reduced in 43%) (Fig. S4 *E and I*) suggest a lack of differentiation in the distal tubules in Invs-Mo–injected embryos, underlining the results obtained for 4A6/3G8 staining.

Two Opposing Directions of Morphogenetic Movements Shape the Early Pronephros. The lack of ventral extension seen after Inversin depletion suggested that Inversin is required for early pronephros morphogenesis. To visualize morphogenetic movements in vivo, we used confocal time-lapse microscopy. Embryos were injected with either CTL-Mo or Invs-Mo in combination with membrane-associated GFP (mem-GFP) and histone-2B–red fluorescent protein (H2B-RFP) to mark the nuclei (Movie S1). Confocal stacks of two embryos were acquired in parallel to synchronously monitor the development of CTL-Mo– vs. Invs-Mo–injected embryos for up to 26 h. Cells clearly identified as part of the pronephros in later time frames were tracked backward to determine their migratory pattern (Movie S2). The calculated trajectories revealed two distinct types of morphogenetic movements (Fig. 2 *A–D*); both elongated the pronephros in a ventral direction. One type of tissue movement originated in the proximal pronephric condensate and extended the tubule in a dorsal to ventral direction (Fig. 2*B*, at 8 h, green, yellow, and red balls). Other cells migrated in a proximal direction, starting from distal parts of the early pronephros (Fig. 2*B*, blue balls). The opposing forces of these two movements extend the primary loop in a ventral direction. Surprisingly, only the dorsal to ventral
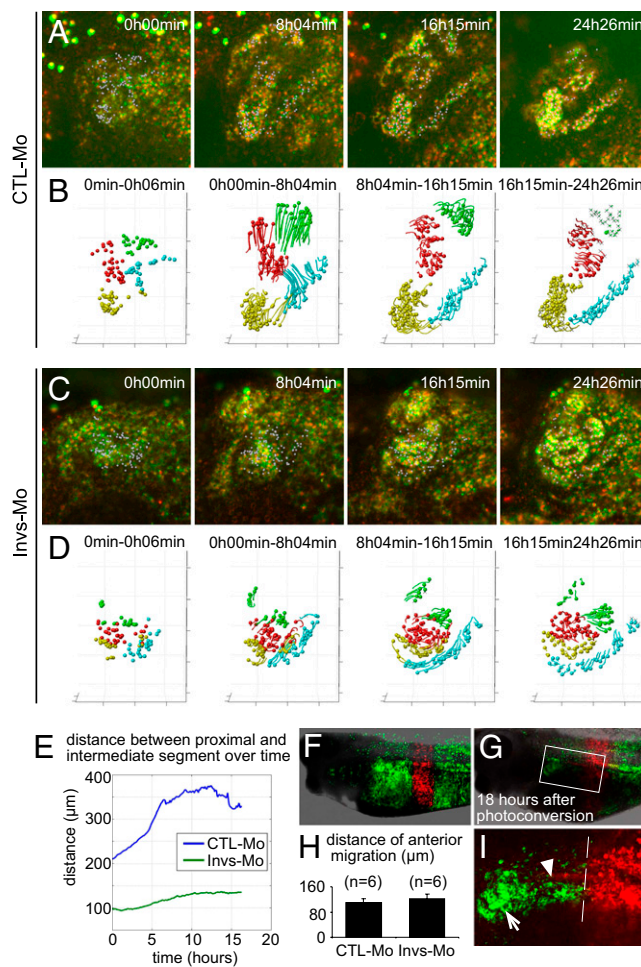
Fig. 2. Inversin affects morphogenetic movements during ventral extension of the proximal pronephros. (*A–E*) Abnormal ventral extension of the Inversin-depleted pronephros. (*A–D*) Time-lapse confocal microscopy of pronephros morphogenesis was performed in parallel between CTL-Mo– and Invs-Mo–injected *Xenopus* embryos to monitor cell movements within the developing proximal pronephros. Cells were labeled by membrane-GFP and nuclear-RFP; only cells clearly identifiable as part of the pronephros were tracked (white dots in *A* and *C*). Clustering of cells with similar movements (green, red, yellow, and blue balls in *B* and *D*) was performed automatically; their trajectories over the indicated time are depicted in *B* and *D*. Cells that left the focal plane are depicted as crosses. (Scale bar: 100 μm.) (*E*) The distance between green (corresponding to the proximal segment) and yellow (intermediate segment) cell clusters in micrometers over time (hours). In contrast to CTL-Mo–injected embryos (blue line), the distance between these two cell clusters failed to increase in Invs-Mo–injected embryos during the first 6 h (green line), causing the abnormal ventral extension of the Inversin-depleted pronephros. (*F–I*) Distal to proximal cell migration is unaffected by Inversin depletion. (*F*) The photo-convertible fluorophore Kaede was broadly expressed in *Xenopus* embryos injected with either CTL- or Invs-Mo. Photoconversion from green to red was restricted to a stripe at stage 34. (*G*) At stage 39 (18 h after photoconversion), red fluorescent cells extended from the red stripe in a proximal direction. (*I*) Enlargement of the boxed area in *G*. The dashed line marks the left-side boundary between the photo-converted area and surrounding tissue. The white arrowhead indicates red fluorescent distal tubule cells that migrated in a proximal direction. The arrow points to the pronephric tubule convolute. (*H*) Measurements of anterior migration in micrometers in CTL- and Invs-Mo–injected *Xenopus* embryos. Error bars represent SEM.

movement originating in the proximal pronephros was severely impaired in the Invs-Mo–injected embryos. The distance of dorsal (green) to ventral (yellow) cell clusters inclined steeply during the first 6 h in CTL-Mo–injected embryos but was reduced in the Invs-

Mo–injected pronephros (Fig. 2*E*). However, the posterior to anterior cell movements remained normal in Invs-Mo–injected embryos (blue balls).

To quantify the role of Inversin in posterior to anterior cell migration, we used a photo-convertible fluorophore (Kaede) (26). Photo conversion was induced at stage 34 in a stripe of 200-μm width and 1.6-mm distance from the head (Fig. 2 *F–I*). After 18–20 h (stages 39 and 40), a stretch of red fluorescent cells was observed that had migrated in a posterior to anterior direction along the pronephric tubule; the migration distance was comparable in Invs-Mo– and CTL-Mo–injected embryos (Fig. 2*H*). Our observation suggests that the cell migration reported in the zebrafish pronephros is conserved in lower vertebrates; however, Inversin is dispensable for this movement.

Proliferation Is Not Affected by Inversin Depletion. Defective dorsal to ventral pronephros extension after Inversin depletion could result from abnormalities in cell proliferation. We performed histological sections on stage 36 embryos and counted proliferating cells marked by positive phospho-Histone H3 staining in the pronephros (Fig. 3*A*). The percentage of mitotic cells was not different on the Invs-Mo–injected side (Fig. 3*B*). To check for increased apoptosis, we performed TUNEL (Fig. 3*D*) and Caspase-3 assays (Fig. 3*E*) (27). Both assays identified apoptotic cells only in the vicinity of the pronephros; the amount of apoptotic cells was not different on the Invs-Mo–injected side.

Camptothecin is a topoisomerase I inhibitor that selectively blocks cell proliferation without affecting cell migration during zebrafish and *Xenopus* embryogenesis (28) (Fig. 3*C*). Embryos were incubated in DMSO or camptothecin during maximal extension of the pronephric loop from stages 31 to 36. The dorsal to ventral dimension of the pronephros was assessed using in situ hybridization for *Na-K-ATPase*. Although the extension of the pronephric loop was intact in camptothecin-treated embryos, total ventral movement was reduced because of the absence of cell proliferation (Fig. 3 *F* and *G*). However, the residual dorsal to ventral extension of the pronephric loop was dramatically reduced by Inversin depletion (Fig. 3*G*, red arrow), confirming that Inversin is required for dorsal to ventral extension of the pronephros independent of proliferation.

Inversin Acts Downstream of Frizzled-8 in Axis Extension and Tubule Development. Frizzled-8 conveys both canonical and noncanonical Wnt signals during early morphogenesis (29–33) and is highly expressed in the developing pronephros (19). The phenotype after knockdown of Frizzled-8 (Fzd-8) closely resembles that of Inversin depletion (19). In Fzd-8–Mo-injected embryos, the pronephric tubule was simplified and shortened (compare Fig. S1*H* and Fig. 4*D*), and the distal and intermediate tubules showed reduced 3G8/4A6 antibody staining (compare Fig. 1*F* and Fig. 4*K*). The extracellular domain of Fzd-8 (ECD-8) acts as a dominant negative, and overexpression leads to convergent extension defects, resulting in a shortened and dorsally bent body axis (30, 31) (Fig. 4*E*). Coexpression of Inversin partially rescued this phenotype, placing Inversin downstream of Fzd-8 in noncanonical Wnt signaling. In a similar fashion, Inversin overexpression rescued the defects in pronephros development caused by Mo-mediated knockdown of Fzd-8 (Fig. 4 *F–N*). These findings indicate that Inversin acts downstream of Fzd-8 during pronephros development.

Inversin depletion did not affect the expression of the canonical Wnt targets *axin2* and *fibronectin* (Fig. S5) detected by in situ hybridization, nor nuclear accumulation of β-Catenin detected by immunostaining (Fig. S6). However, combined depletion of Dishevelled-1 and -3 or coexpression of the dominant-negative Dishevelled mutant Xdd1, interfering with PCP signaling (34), mimicked the phenotype of Invs-Mo injection (Fig. S6 *C–F*). Because phospho-JNK1/2 was localized at comparable levels with the
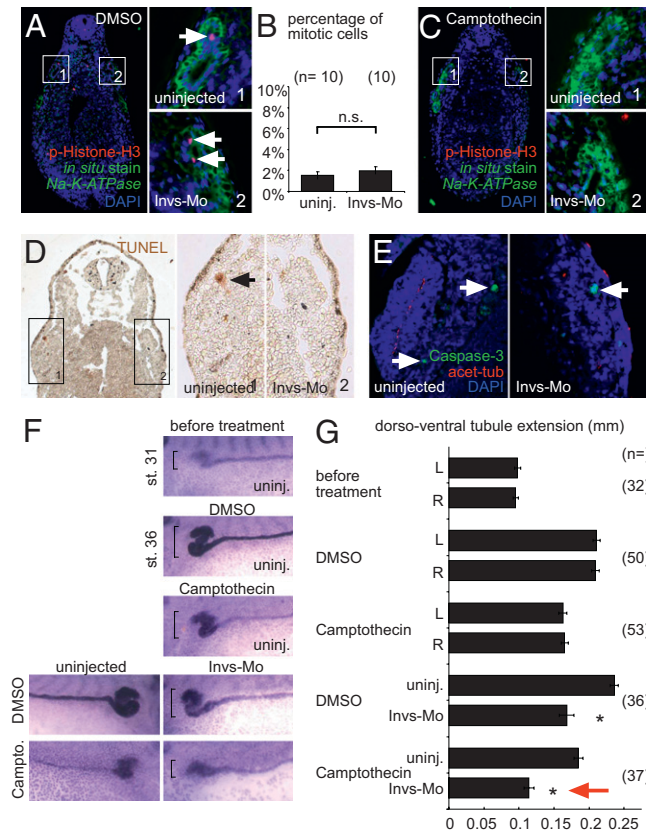
Fig. 3. Impaired pronephros morphogenesis caused by Inversin depletion is largely independent of proliferation or apoptosis. (*A*) Embryos were in situ hybridized against *Na-K-ATPase* (inverted differential interference contrast, green) and immunostained with an anti–phospho-Histone H3 (p-Histone H3) antibody (red) and DAPI (blue). The area of the proximal pronephros was magnified (*Right*). (*B*) The percentage of mitotic (p-Histone H3-positive) cells in the pronephros was determined in five sections of 10 embryos; no significant difference was detected ($P = 0.36$, Student *t* test). (*C*) Section of a camptothecin-treated embryo; camptothecin almost completely abrogates mitosis. The area of the proximal pronephros was magnified (*Right*). (*D*) Positive TUNEL staining is indicated by a black arrow. The area of the proximal pronephros was magnified (*Right*). (*E*) Immunostaining with anti–Caspase-3 (green), acetylated tubulin (red), and DAPI (blue). Note that both methods did not detect increased apoptosis on the Invs-Mo–injected side. (*F* and *G*) Mitotic inhibition does not prevent ventral extension defects of pronephric loops after Invs-Mo injection. (*F*) Embryos were treated at stage 31 with DMSO or camptothecin and processed for in situ hybridization against *Na-K-ATPase* at stage 36. Brackets mark the boundaries of ventral extension of the pronephric loop. (*G*) Quantification of ventral extension in millimeters. Error bars represent SD (*$P < 0.001$). The red arrow points to a reduction of the ventral pronephros extension in Invs-Mo–injected embryos that significantly exceeds the reduction caused by camptothecin treatment alone.

nuclei of both uninjected and Invs-Mo–injected pronephroi (Fig. S7B) and the mixed lineage serine/threonine kinase 2 (MLK2), an upstream activator of JNK expressed in the pronephros (35), did not rescue the Invs-Mo phenotype (Fig. S7C), the function of Inversin during pronephros formation does not seem to involve JNK activation.

Normal Localization of Dishevelled in Ectodermal and Tubular Epithelial Cells Requires Inversin. Recruitment of Dishevelled to the plasma membrane in response to Frizzled receptors is a key event in noncanonical Wnt signaling (6, 7). To investigate whether the membrane localization of Dishevelled in response to Fzd-8 depends on Inversin, we used sequentially injected ectodermal explants (animal caps) to generate mosaic cell clusters (Fig. 5A). The first injection into two cell-stage embryos directed the ex-
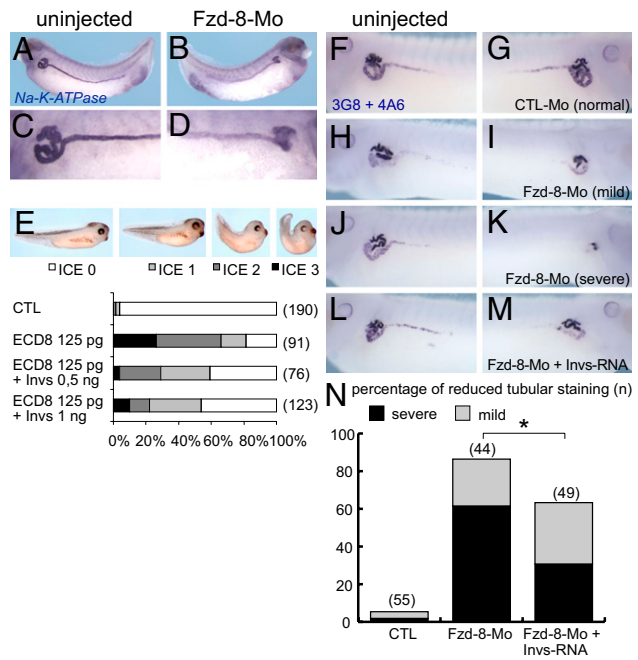

Fig. 4. Inversin acts downstream of Frizzled-8 in convergent extension movements and pronephros development. (*A*–*D*) Embryos were unilaterally injected with Fzd-8–Mo. In situ hybridization against *Na-K-ATPase* shows reduced ventral extension of the intermediate tubule. (*C* and *D*) Enlarged view of the pronephros region in *A* and *B*. (*E*) Dorsal injection of dominant-negative *Xenopus* Frizzled-8 encompassing the extracellular domain of Frizzled-8 (ECD8). Axis extension defects indicative of impaired convergent extension (ICE) were scored as indicated on a scale from 1 to 3. Coexpression of Inversin mRNA partially rescued the convergent extension defects. (*F*–*N*) Staining of the pronephros with the tubule-specific antibodies 3G8 and 4A6. (*H*–*M*) Unilateral injection of Fzd-8–Mo resulted in a reduction of 3G8 and 4A6 staining ranging from mild (*I*) to severe (*K*). (*L*–*N*) Coinjection of Inversin mRNA (1 ng) rescued the defective 3G8/4A6 immunoreactivity in Fzd-8–Mo-injected embryos (*$P < 0.05$).

pression of Dishevelled-GFP to all ectodermal cells. The second injection targeted a subset of cells; a nuclear marker (H2B-RFP) was included to track the second injection. Dishevelled-GFP alone predominantly formed punctuated aggregates in the cytoplasm (Fig. 5B). If Fzd-8 was included in the second injection, Dishevelled-GFP localized to the plasma membrane (Fig. 5B). Invs-Mo injection dramatically diminished the translocation of Dishevelled-GFP to the membrane; instead, Dishevelled-GFP accumulated diffusely in the cytoplasm (Fig. 5C). Cytoplasmic Dishevelled-GFP was hardly detectable at microscope settings used to image the membrane-bound Dishevelled-GFP in mosaic tissues (Fig. S8G for Dishevelled-GFP localization in nonmosaic explants). Dishevelled-GFP membrane recruitment was restored in cells expressing mouse Inversin, resistant to Invs-Mo (Fig. 5D). These experiments show that Inversin is essential for the translocation of Dishevelled in response to Fzd-8. To analyze whether Inversin directs the localization of Dishevelled during pronephros formation, we examined the subcellular localization of endogenous Dishevelled in stage-36 embryos (Fig. 5 *E* and *F*). Embryos, injected unilaterally with Invs-Mo, were labeled with antiserum against Dishevelled-2 as well as acetylated α-tubulin to identify the cilia of the pronephric tubules. On the uninjected side, Dishevelled was detected at the apical membrane of pronephric tubules (Fig. 5E). In the Invs-Mo–injected side, staining for endogenous Dishevelled was strongly reduced or not detectable at the apical membrane (Fig. 5F). These findings indicate that Inversin regulates Dishevelled localization during *Xenopus* pronephros development.
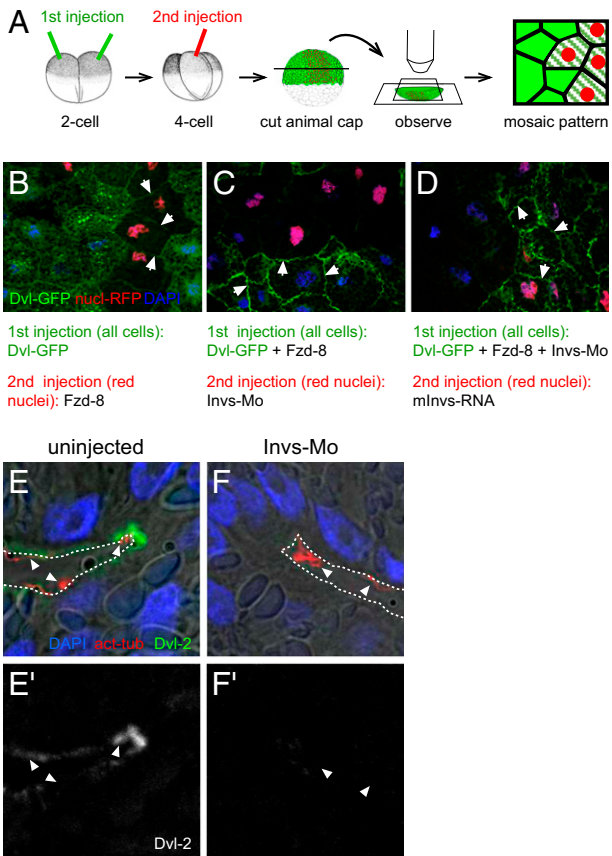
Fig. 5. Inversin is required for membrane localization of Dishevelled. (*A*) Mosaic cell clusters in animal caps were generated by sequential injection at the two- and four-cell stage. All cells received a first injection at the two-cell stage that included Dishevelled-GFP. A subset of these cells received a second injection at the four-cell stage; only cells modified by the second injection are marked by red nuclei expressing histone-2B–red fluorescent protein (H2B-RFP). Thus, neighboring mosaic cell clusters with different injections can be compared based on the presence or absence of red nuclei. (*B*) Dishevelled-GFP, localized in a typically punctuate pattern (first injection, all cells), is recruited to the plasma membrane in Frizzled-8 (Fzd-8)–injected cells (second injection, cells with red nuclei). (*C*) Fzd-8–induced membrane localization of Dishevelled (first injection, all cells) is abolished in the subset of cells that received the Invs-Mo in a second injection (second injection, cells with red nuclei). (*D*) Defective membrane recruitment of Dishevelled after injection of Dishevelled-GFP, Fzd-8, and Invs-Mo (first injection, all cells) can be rescued by mouse Inversin RNA injection (second injection, cells with red nuclei). DAPI staining (blue) visualizes all cell nuclei. White arrows point to membrane-localized Dishevelled. (*E* and *F*) In immunostaining of stage-36 embryos, Dishevelled-2 (green) localizes to the membrane of tubular epithelial cells indicated by the presence of cilia (acetylated tubulin in red, white arrowheads). A dashed line indicates the apical surface of the pronephric tubule; nuclei are stained with DAPI (blue). The Invs-Mo–injected side shows a strong reduction of Dishevelled-2 staining at the apical membrane of the pronephric tubules. The Dishevelled channel is depicted alone in *E'* and *F'*.

Discussion

In vivo imaging of intact *X. laevis* embryos allowed us to follow the extension and convolution of the proximal *Xenopus* pronephros. Two opposing morphogenetic cell movements shape the primary loop, which continues to form the intermediate segment. Inversin is required for the dorsal to ventral movement of the proximal pronephros but not for the posterior to anterior movement originating in the distal pronephros. Remarkably, the morphogenetic cell movements of the proximal tubule precede the onset of filtration and a fully functional pronephric system at Nieuwkoop-Faber stage 37/38 (12). Thus, fluid flow, which is a driving force for the collective distal to proximal cell migration observed in zebrafish pronephros development (28), is clearly not needed for the initial configuration of the proximal *Xenopus* pronephros, but it may contribute to the lengthening, extension, and differentiation of the pronephric convolute at later stages.

Although Inversin-depleted tubules seem to encompass fewer cells, we did not detect changes in either mitosis or apoptosis. However, we cannot exclude differences in proliferation or apoptosis during earlier stages. Alternatively, abnormal morphogenetic movements might change the fate of cells, preventing their participation in pronephros morphogenesis.

Our findings suggest that Inversin promotes the translocation of Dishevelled in response to Frizzled receptors. Inversin alone does not recruit Dishevelled to the plasma membrane (Fig. S3), revealing the importance for upstream components such as Frizzled receptors. Nevertheless, our results identify Inversin as one of the few known molecules that link Dishevelled to Frizzled receptors. Inversin shares the overall domain architecture with the *Drosophila* protein Diego; Diego interacts with Dishevelled and stabilizes the Frizzled/Dishevelled complex at the plasma membrane (3). Whether Inversin stabilizes or actively recruits Dishevelled to the plasma membrane requires further investigation. Contributing to our understanding of the molecular pathogenesis of NPH, our results show that Inversin acts downstream of Frizzled-8, a receptor implicated in the transmission of noncanonical Wnt/PCP signaling events, to facilitate the extension and subsequent elongation of the tubular system in the *Xenopus* pronephros.

In contrast to the knockdown of Polycystin-2 or Bicaudal C (36), we did not observe tubule dilation in the *Xenopus* pronephros after knockdown of Inversin (Fig. S1*G*). Instead, Inversin depletion caused severe edema, potentially because of impaired water elimination. We speculate that simplification of the proximal pronephros convolute and shortening of the intermediate segment reduce the efficiency of fluid excretion. The *Xenopus* pronephros actively excretes water, whereas the mammalian kidney faces the opposite task of water conservation (37, 38). A concentration defect is one of the clinical manifestations in human NPH. Most of the glomerular ultrafiltrate is reabsorbed in the proximal tubule and loop of Henle, the segment that corresponds to the intermediate tubule in *Xenopus* embryos. The interstitium occupying the space in between proximal tubular segments of Inversin-deficient (*inv*) mice is disorganized and more abundant (39). Analysis of the ClC-K_a–positive nephron segments of *inv*($^{-/-}$) mice (Fig. S2 *K–M*) supports the hypothesis that defective elongation of the proximal nephron segments occurs in human disease and may account for the widened interstitium in *inv* mice. The observed reduction in nephron number may contribute to the phenotype. Interestingly, 20% of patients with a mutation in *Invs/NPHP2* have smaller kidneys in renal ultrasound (40). Thus, abnormal cell migration and nephron differentiation may contribute to the renal manifestations of NPH.

Materials and Methods

Embryos were cultured and manipulated as described (12, 41). All experiments were approved by the institutional animal committee (Regierungspräsidium Baden Württemberg). Invs-Mo (GeneTools): 5′-GGCTACTCATACTAGAACTGG-GACA-3′; Fzd-8–Mo: 5′- GCAGCGACAGCGACAGACTCTCCAT-3′. Standard methods for staining and in situ hybridization were used (42). For tubular excretion assay, 10–40 nL 70-kDa FITC dextran (Molecular Probes) were injected. A Zeiss LSM 5 LIVE DuoScan with a motorized stage was used for parallel imaging at separate locations at 3-min intervals and photoconversion of Coral Hue Kaede (26). Motion in the 4D data was analyzed with a variational optical flow approach.

Embryos were incubated in 60 μM Camptothecin (C9911; Sigma) in 1% DMSO. A detailed description of reagents, embryo manipulations, migration assays, and statistical analysis can be found in *SI Materials and Methods*.

1. Simons M, Walz G (2006) Polycystic kidney disease: Cell division without a c(l)ue? *Kidney Int* 70:854–864.
2. Benzing T, Simons M, Walz G (2007) Wnt signaling in polycystic kidney disease. *J Am Soc Nephrol* 18:1389–1398.
3. Feiguin F, Hannus M, Mlodzik M, Eaton S (2001) The ankyrin repeat protein Diego mediates Frizzled-dependent planar polarization. *Dev Cell* 1:93–101.
4. Das G, Jenny A, Klein TJ, Eaton S, Mlodzik M (2004) Diego interacts with Prickle and Strabismus/Van Gogh to localize planar cell polarity complexes. *Development* 131:4467–4476.
5. Simons M, et al. (2005) Inversin, the gene product mutated in nephronophthisis type II, functions as a molecular switch between Wnt signaling pathways. *Nat Genet* 37:537–543.
6. Axelrod JD, Miller JR, Shulman JM, Moon RT, Perrimon N (1998) Differential recruitment of Dishevelled provides signaling specificity in the planar cell polarity and Wingless signaling pathways. *Genes Dev* 12:2610–2622.
7. Park TJ, Gray RS, Sato A, Habas R, Wallingford JB (2005) Subcellular localization and signaling properties of dishevelled in developing vertebrate embryos. *Curr Biol* 15:1039–1044.
8. Otto EA, et al. (2003) Mutations in INVS encoding inversin cause nephronophthisis type 2, linking renal cystic disease to the function of primary cilia and left-right axis determination. *Nat Genet* 34:413–420.
9. Mochizuki T, et al. (1998) Cloning of inv, a gene that controls left/right asymmetry and kidney development. *Nature* 395:177–181.
10. Morgan D, et al. (1998) Inversin, a novel gene in the vertebrate left-right axis pathway, is partially deleted in the inv mouse. *Nat Genet* 20:149–156.
11. Saxén L, Sariola H (1987) Early organogenesis of the kidney. *Pediatr Nephrol* 1:385–392.
12. Nieuwkoop PD, Faber J (1994) *Normal Table of Xenopus Laevis (Daudin)* (Garland, New York).
13. Raciti D, et al. (2008) Organization of the pronephric kidney revealed by large-scale gene expression mapping. *Genome Biol* 9(5):R84.
14. Vize PD, Jones EA, Pfister R (1995) Development of the Xenopus pronephric system. *Dev Biol* 171:531–540.
15. Jones EA (2005) Xenopus: A prince among models for pronephric kidney development. *J Am Soc Nephrol* 16:313–321.
16. Reggiani L, Raciti D, Airik R, Kispert A, Brändli AW (2007) The prepattern transcription factor Irx3 directs nephron segment identity. *Genes Dev* 21:2358–2370.
17. Cornish JA, Etkin LD (1993) The formation of the pronephric duct in Xenopus involves recruitment of posterior cells by migrating pronephric duct cells. *Dev Biol* 159:338–345.
18. Karner CM, et al. (2009) Wnt9b signaling regulates planar cell polarity and kidney tubule morphogenesis. *Nat Genet* 41:793–799.
19. Satow R, Chan TC, Asashima M (2004) The role of Xenopus frizzled-8 in pronephric development. *Biochem Biophys Res Commun* 321:487–494.
20. Tran U, Pickney LM, Ozpolat BD, Wessely O (2007) Xenopus Bicaudal-C is required for the differentiation of the amphibian pronephros. *Dev Biol* 307:152–164.
21. McCoy KE, Zhou X, Vize PD (2008) Collectrin/tmem27 is expressed at high levels in all segments of the developing Xenopus pronephric nephron and in the Wolffian duct. *Gene Expr Patterns* 8:271–274.
22. Demartis A, Maffei M, Vignali R, Barsacchi G, De Simone V (1994) Cloning and developmental expression of LFB3/HNF1 beta transcription factor in Xenopus laevis. *Mech Dev* 47:19–28.
23. Brennan HC, Nijjar S, Jones EA (1998) The specification of the pronephric tubules and duct in Xenopus laevis. *Mech Dev* 75:127–137.
24. Heller N, Brändli AW (1999) Xenopus Pax-2/5/8 orthologues: Novel insights into Pax gene evolution and identification of Pax-8 as the earliest marker for otic and pronephric cell lineages. *Dev Genet* 24:208–219.
25. Chan TC, Takahashi S, Asashima M (2000) A role for Xlim-1 in pronephros development in Xenopus laevis. *Dev Biol* 228:256–269.
26. Ando R, Hama H, Yamamoto-Hino M, Mizuno H, Miyawaki A (2002) An optical marker based on the UV-induced green-to-red photoconversion of a fluorescent protein. *Proc Natl Acad Sci USA* 99:12651–12656.
27. Tseng AS, Adams DS, Qiu D, Koustubhan P, Levin M (2007) Apoptosis is required during early stages of tail regeneration in Xenopus laevis. *Dev Biol* 301:62–69.
28. Vasilyev A, et al. (2009) Collective cell migration drives morphogenesis of the kidney nephron. *PLoS Biol* 7:e9.
29. Itoh K, Jacob J, Y Sokol S (1998) A role for Xenopus Frizzled 8 in dorsal development. *Mech Dev* 74:145–157.
30. Deardorff MA, Tan C, Conrad LJ, Klein PS (1998) Frizzled-8 is expressed in the Spemann organizer and plays a role in early morphogenesis. *Development* 125:2687–2700.
31. Itoh K, Sokol SY (1999) Axis determination by inhibition of Wnt signaling in Xenopus. *Genes Dev* 13:2328–2336.
32. Wallingford JB, Vogeli KM, Harland RM (2001) Regulation of convergent extension in Xenopus by Wnt5a and Frizzled-8 is independent of the canonical Wnt pathway. *Int J Dev Biol* 45:225–227.
33. Takada R, Hijikata H, Kondoh H, Takada S (2005) Analysis of combinatorial effects of Wnts and Frizzleds on beta-catenin/armadillo stabilization and Dishevelled phosphorylation. *Genes Cells* 10:919–928.
34. Sokol SY (1996) Analysis of Dishevelled signalling pathways during Xenopus development. *Curr Biol* 6:1456–1467.
35. Poitras L, Bisson N, Islam N, Moss T (2003) A tissue restricted role for the Xenopus Jun N-terminal kinase kinase kinase MLK2 in cement gland and pronephric tubule differentiation. *Dev Biol* 254:200–214.
36. Tran U, et al. (2010) The RNA-binding protein bicaudal C regulates polycystin 2 in the kidney by antagonizing miR-17 activity. *Development* 137:1107–1116.
37. Grantham JJ, Wallace DP (2002) Return of the secretory kidney. *Am J Physiol Renal Physiol* 282:F1–F9.
38. Gusmano R, Ghiggeri GM, Caridi G (1998) Nephronophthisis-medullary cystic disease: Clinical and genetic aspects. *J Nephrol* 11:224–228.
39. Phillips CL, et al. (2004) Renal cysts of inv/inv mice resemble early infantile nephronophthisis. *J Am Soc Nephrol* 15:1744–1755.
40. Tory K, et al. (2009) Mutations of NPHP2 and NPHP3 in infantile nephronophthisis. *Kidney Int* 75:839–847.
41. Newport J, Kirschner M (1982) A major developmental transition in early Xenopus embryos: I. Characterization and timing of cellular changes at the midblastula stage. *Cell* 30:675–686.
42. Sive HL, Grainger RM, Harland RM (2000) *Early Development of Xenopus laevis: A Laboratory Manual* (Cold Spring Harbor Laboratory Press, Plainview, NY).

DEVELOPMENTAL BIOLOGY